International Journal of Engineering and Advanced Technology (IJEAT)
ISSN: 2249-8958 (Online), Volume-9 Issue-1, October, 2019

Deep Learning Based Depthwise Separable Model For Effective Diagnosis And Classification of Lung Ct Images

D. Jayaraj, S. Sathiamoorthy

Abstract: ***Lung cancer is a serious illness which leads to increased mortality rate globally. The identification of lung cancer at the beginning stage is the probable method of improving the survival rate of the patients. Generally, Computed Tomography (CT) scan is applied for finding the location of the tumor and determines the stage of cancer. Existing works has presented an effective diagnosis classification model for CT lung images. This paper designs an effective diagnosis and classification model for CT lung images. The presented model involves different stages namely pre-processing, segmentation, feature extraction and classification. The initial stage includes an adaptive histogram based equalization (AHE) model for image enhancement and bilateral filtering (BF) model for noise removal. The pre-processed images are fed into the second stage of watershed segmentation model for effectively segment the images. Then, a deep learning based Xception model is applied for prominent feature extraction and the classification takes place by the use of logistic regression (LR) classifier. A comprehensive simulation is carried out to ensure the effective classification of the lung CT images using a benchmark dataset. The outcome implied the outstanding performance of the presented model on the applied test images.***

Keywords: Lung cancer; CT images; Feature extraction; Classification; Segmentation.

I. INTRODUCTION

Lung cancer is a major reason for the mortality rate due to cancer among men as well as women. It is reported that around 1 million patients are identified with lung cancer annually and 90% of them died [1]. The chance of living is maximum when the detection of cancer takes place at the beginning level. However, the earlier identification is also not an easier process. Computer-aided diagnosis model finds useful for the professionally to detect and diagnose the abnormal images at the early stage and quickly. Generally, lung cancer is considered as a severe issue when compared to other diseases and is mostly identified by the medical centres [2]. If the disease is diagnosed in early stage, then it can increase the lifetime of a person. Identifying the lung cancer in primary stage is not a simple assignment. In most of the cases, the disease is diagnosed in a chronic stage. In all over the world, lung cancer has secured second position among male and tenth among female. Regarding the details given in these work is only a hint given about lung cancer that consist of 4 main phases. The lung cancer is placed as frequently occurring cancer in female subsequent to breast cancer as well as colorectal cancer [3]. Feature extraction offers a simple and effective dimensionality reduction technique in image related processes. The non-obtrusive behaviour is an outstanding characteristic in CT images. The filtered features subset takes only the related data from input to the reduction procedure. The reduced features are used by support vector machine (SVM) to train as well as test the model. They are utilized to classify lung images through neural network (NN) scheme with binarization image pre-processing. The current study related to classifying lung cancer images is done by the use of a NN model that offers 80% of accuracy. Diverse analysis has been carried out related to lung cancer classification. SVM is one of the universal learning techniques that depend on statistical learning hypothesis. But, the method used is very expensive and to detect lung cancer in primary stage that has minimum survival rate of human beings. The premature recognition of cancer is helpful to cure the disease completely. Hence, there is a need of designing the method of predicting the cancer nodules in the untimely stage is raising.

Cause and identification of lung cancer

- Common deduction of lung cancer is not possible as professionals are not able to identify the affected area unless it reaches the chronic stage. The survival rate may be increased to additional 5 years if the disease is deducted in primary phase, else it would be complex when it reaches propelled stage.
- One main reason for lung cancer is smoking; physicians had concluded that chain smokers and long time smokers have the vulnerability of lung cancer. They also state that there is no other reason to affect by lung cancer.

Revised Manuscript Received on October 30, 2019.
* Correspondence Author
D. Jayaraj, Department of Computer Science & Engineering, Annamalai University, Chidambaram. Email: jayarajvnr@gmail.com
S. Sathiamoorthy, Tamil Virtual Academy, Chennai. Email: ks_sathia@yahoo.com

- To deduct lung cancer, persons take X-ray or CT or MRI scans to decide any abnormal development in lung areas. In such cases, unusually sensitive CT could discover small lumps that possibly be a cancer.
- Identification of the cancer in the initial stage:
- The earlier finding of lung cancer helps to increase the lifetime rate of human beings by undergoing many other treatments and diagnosis. Aside, considerable human beings can be treated only if diagnosing is one in earlier stage.

[4] suggested a model lung cancer classification which tracks the Texture, Shape and Deep model-learned data (Fuse-TSD) in the deciding stage. It uses a GLCM-based surface descriptor, a Fourier-shape descriptor to depict the heterogeneity of nodules and a DCNN to teach the features of nodes. [5] examined a framework called CAD that depends on CNN to categorize the breast cancer. Deep learning method usually involves in expandable datasets to arrange systems during the transfer learning method that utilizes small datasets of medical figures. The CNN is trained in a reputed form using the transfer learning approach. The CNN achieved the best results in terms of accuracy i.e., 98.94%. [6] has shown the demonstration of the DNN classifier to classify the brain tumor, where the DNN is integrated to wavelet transform and principal component analysis.

[7] presented a technique called regularized linear discriminant analysis where regularization parameter has been operated in conventional cross validation model. For exploring the medicinal details, the forecast of disease requires an appropriate feature subset. Various evolutionary techniques have been used to attain the best choice of features. At recent times, gravitational search algorithm as well as Elephant Herd optimization which are used to choose optimum features [8, 9]. [10] designed a ANN based model to classify the CT cancer images. The statistical use of the classifier technique is designed and states that feed forward back propagation network offered improved results.

[11] presented a summed up LDA method is projected which depends on Euclidean norm known as ELDA technique to overcome the present limitations or drawbacks that is present in the classical LDA process. A Multi-class SVM is linked for executing the step classification. This method exhibits that this algorithm achieves enhanced outcome with similar accuracy, viability when compared to many other procedures or scheme.

This paper designs an effective diagnosis and classification model for CT lung images. The presented model involves different stages namely pre-processing, segmentation, feature extraction and classification. The earlier stage includes an adaptive histogram based equalization (AHE) model for image enhancement and bilateral filtering (BF) model for noise removal. The pre-processed images are fed into the second stage of watershed segmentation model for effectively segment the images. Then, a deep learning based Xception model is applied for prominent feature extraction and the classification takes place by the use of logistic regression (LR) classifier. A comprehensive simulation is carried out to ensure the effective classification of the lung CT images using a benchmark dataset. The outcome implied the outstanding performance of the presented model on the applied test images.

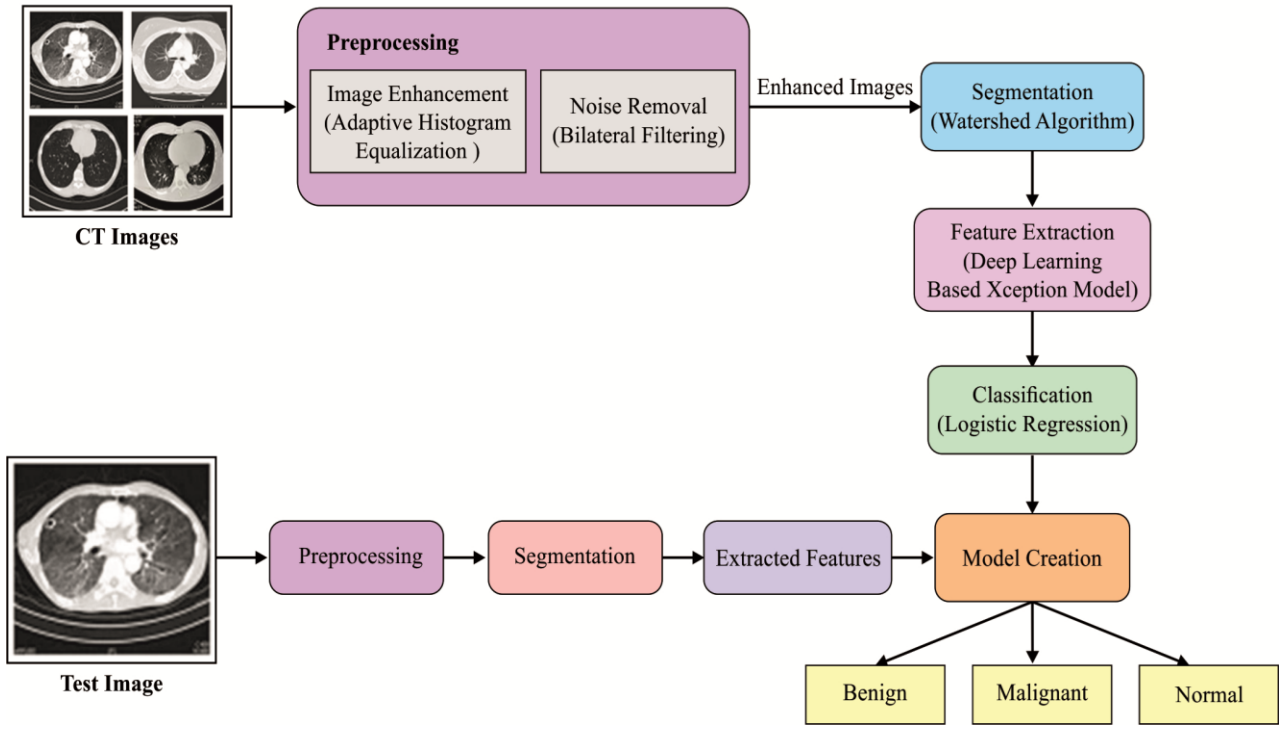

Fig. 1. Working procedure of presented model

PROPOSED MODEL

The overall process is clearly illustrated in Fig. 1. Initially, the images undergo pre-processing stage for improvising the quality and eliminate the noises exist in the image. Then, the images are segmented using the watershed algorithm. Then, a deep learning based Xception model is applied for prominent feature extraction and the classification takes place by the use of logistic regression (LR) classifier. The outcome from the classification model indicates whether the input CT lung image has cancer or not.

A. Pre-processing

In this paper, the pre-processing takes place in two levels namely image enhancement using AHE and noise removal using BF. At the beginning, AHE model is utilized because of its advantages namely effectiveness and low complexity. It improvises the image quality and visual effect by enlarging the distribution of grayscale values present in the image. It is mainly depends upon the probability distribution function. It resolves the difficulties present in conventional models through the automatic detection and adaptable nature to the grayscale images.

At the second level, BF is employed on the CT images in grayscale form. Normally, few amount of noise is presented at the CT image production which might results to the false identification of cancer nodules. So, it is needed to effectively identify the noise prior to classification. The idea of BF depends upon a selective weighting mechanism for averaging adjacent pixels for removing the noises. The common way of representing BF comprises a distance based domain filter part (i, i'), and a gray-value dependent range filter part $r((f\,i),(f\,i'))$:

$$\tilde{f}(i) = \frac{1}{N(x)} \int_{-\infty}^{\infty} f(i') d(i,i') r\Big(f(i), f(i')\Big) di' \qquad (1)$$

Where i indicates the location of the middle pixel, i' represents the location of adjacent pixels, and $N(i)$ a normalization factor. When the domain filter considers a local averaging of adjacent pixels, the range filter part forces the value based element to eliminate the filtering between the edges. For domain and range filter regions, generally, a Gaussian function is employed and is based on the Euclidean pixel distance as given below.

$$d(i,i') \propto \exp\left(-\frac{(i-i')^2}{2\sigma_d^2}\right) \qquad (2)$$

$$r\Big(f(x), f(x')\Big) \propto exp\left(-\frac{\big(f(x)-f(x')\big)^2}{2\sigma_f^2}\right) \qquad (3)$$

with σ_d is a width parameter of the filter kernel size and σ_f the noise standard deviation of the assumed reconstruction value (e.g. attenuation noise standard deviation σ_a)

B. Watershed based image segmentation

This technique [12] assumes a figure as a topographic landscape with ridges as well as valleys. The height value of the landscape is widely viewed by the gray values of the specific pixels or the gradient magnitudes. Based on 3D view of the watershed transform, decomposition of images takes place using a collection of catchment basins. In each local minima, the catchment basin comprises the root whose route of steepest descent end at the minima is depicted in Fig. 2. The watershed transform performance provides the entire decomposition of an image as well as allocating each pixel to a portion or watershed. With respect to noisy medicinal images, huge count of small regions is created that is considered as a problem of over segmentation. If image segmentation is to be performed, then the feature extraction procedure is necessary.

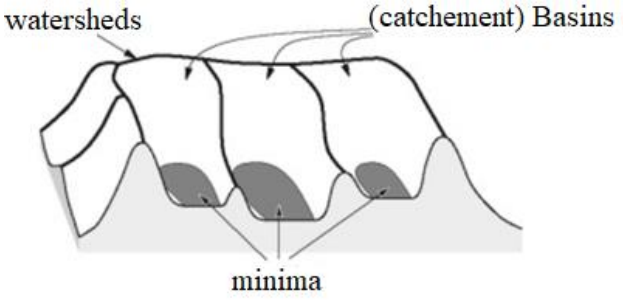

Fig. 2. Concept of watershed transform

For efficient extraction of features, it is very important to group the voxel wise morphometric features to regional features which holds high dimensional features involving a huge count of repeated or unnecessary data as well as noise due to the existence of error in the registration procedure. Simultaneously, the utilizing the regional features can reduce this problem as well as to provide healthier features in the classifier process. A conventional approach to attain the regional features is to utilize former knowledge, i.e. fixed ROI that review each voxel-wise features in each fixed ROI. But, it is not so effective while utilization of several templates to symbolize MV images, as the ROI features from other templates are more common. To capture different types of various MV features from other templates, a clustering technique is deployed for dynamic grouping of features. It states that the utilization of clustering model improves the discriminative power of the acquired regional features, and reduce the bad influence from the registration error.

Let $\boldsymbol{I_i^j(v)}$ denotes a voxel-wise cell thickness value at voxel u in the kth template for the ith training subject, $\boldsymbol{i \in [1, N]}$. The ROI part for the kth template is based on the incorporated discrimination and robustness metric, $\boldsymbol{DRM^j(v)}$, concluded from all the N training subjects that assumes the feature significance and spatial reliability into account. It is viewed as follows.

$$DRM^j(v) = P^j(v)C^j(v) \quad (4)$$

where $P^j(v)$ is the voxel-wise Pearson correlation (PC) from each individual N training subjects, and $C^j(v)$ indicates the spatial steadiness among every feature in the spatial neighbourhood. Watershed segmentation is processed on every computed DRM^j map to attain the ROI region for the kth template. In noticing the Gaussian kernel is used for smoothing all maps DRM^j to avoid over segmentation. As a result, the k[th] template could be splitted to a total R^j non overlapping areas; it should be noticed that all template offers an output under individual ROI region.

C. Xception model based feature extraction

Xception model is designed by Chollet [13], who developed the Keras library. It is an extended model of Inception which undergoes a replacement with the conservative Inception module using depth-wise separable convolution.

- CNN, specifically, VGG-16 architecture that is illustrated identically to the proposed approach in some feature.
- The Inception architecture family of CNN shows the advantages of factoring convolution into several other modules to be operated in series on channels and space.

Depth wise independent convolution is used in the proposed Xception approach. Though the practice of using spatially divisible convolution in CNN is from earlier stage, the depth wise version is the improved technique. In 2013, Laurent Sifre established this depth wise separable convolution approach during the training period at Google Brain, and deployed it in AlexNet to get minor development with respect to gain and high improvement in terms of convergence speed, and considerable reduction in the size of the approach. The initial approach on depth wise separable convolution depends on the earlier study on transformation invariant scattering. Then, a depth wise separable convolution is applied as the primary layer of Inception V1 as well as V2.

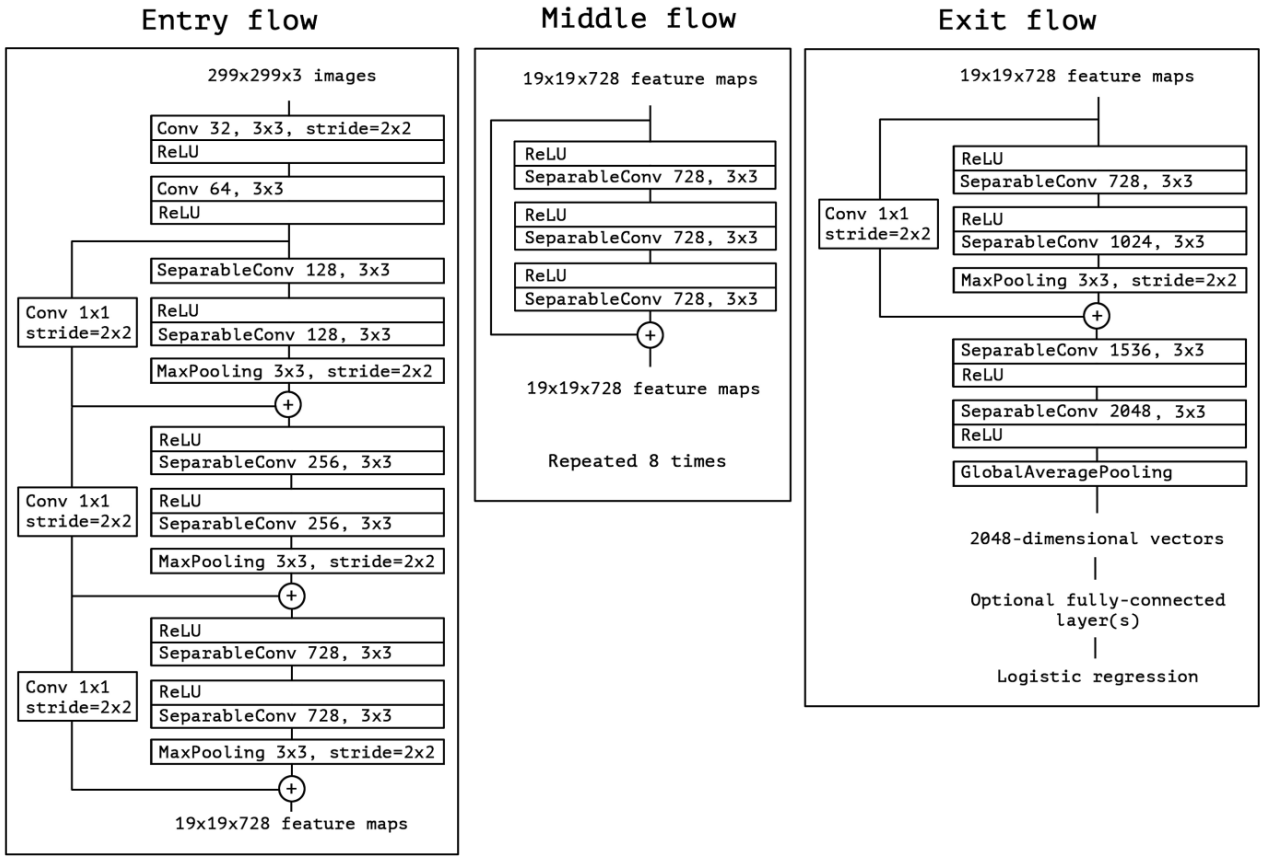

Fig. 3. Xception architecture

1. Architecture

The structure of CNN is mainly based on depth-wise separable *conv layers* that is offered. The set of following assumption is prepared that match the cross-channels as well as spatial correlation in the feature maps of CNN that is entirely decoupled. Because of this fact an efficient hypothesis is presented using basic Inception architecture, the proposed Xception technique denotes "Extreme Inception" and corresponding units are clear which is depicted in Fig. 3. The Xception model comprises of 36 convolutional layers that constructs the feature extracting base of the network. In simulation part, image classification is done by investigating as well as convolutional base is pursued by a logistic regression layer. It is not mandatory that the entirely connected layers should be included at the earlier stage to the logistic regression layer.

There are 36 convolutional layers which are arranged into 14 components, each unit consist of linear remaining correlations around them leaving the initial and final modules. In short, the Xception architecture has a linear stack of depth wise independent conv layers with left over links. These features are helpful in terms of easy description as well as for modification. It requires only less number of coding that is from the high level library like Keras or TensorFlow-Slim, distinctly to the models such as VGG-16, but the accessible Inception V2 or V3 techniques are not so easy to describe.

2. Xception as feature extractor

Xception comes from the Inception model which undergoes replacement using depth wise separable convolutions. It has approximately identical parameter count as Inception-v1 model. Convolution and pooling is applied for automatically extract as well as reduce the features. Assume an image X of size (i, j), the representation of convolution takes place as follows.

$$C(i,j) = (I * w)(i,j) = \sum_k \sum_l I(i-k, j-l) w(k,l) \qquad (5)$$

where w is the convolution kernel size of (k, l). The convolution provides a solution of learning the images and the parameter sharing minimizes the model complexity. Pooling acts as a process of reducing the features. It assumes a collection of nearby pixels in the feature map and creates a value for representation as depicted in Fig. 4.

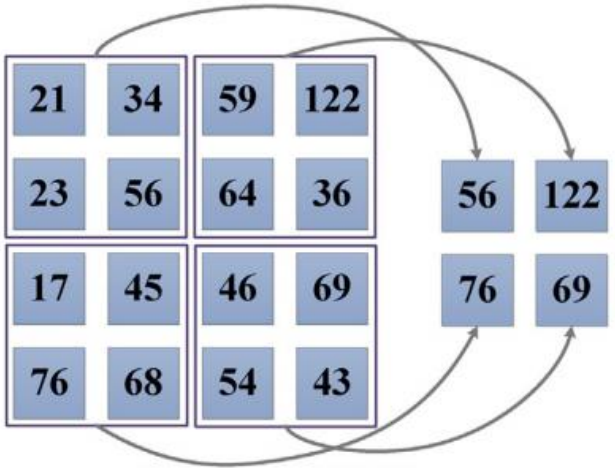

Fig. 4. Max Pooling

The feature map is defined as 4 × 4, the max pooling creates a maximum value in each 2 × 2 block that minimizes the feature dimension considerably. Cross channel normalization comes under a local normalization model which enhances the generalization. The feature maps undergo normalization in prior to feed to the subsequent layers. The Cross channel normalization provides a sum from diverse adjacent maps at the identical location. This process can be seen in the real neurons.

D. LR based classification

LR is a popular machine learning model generally applied to classify the data. The logistic distribution offers the fundamental to the logit model with its distribution function as given in Eq. (6).

$$F(X_k\beta) = \frac{\exp(X_k\beta)}{1 + exp(X_k\beta)} \qquad (6)$$

and its density function can be defined as Eq. (7).

$$F(X_k\beta) = \frac{\exp(X_k\beta)}{[1 + exp(X_k\beta)]^2} \qquad (7)$$

II. EXPERIMENTAL VALIDATION

In this study, a benchmark lung cancer CT image dataset is utilized which comprises a set of fifty 50 low-dosage images [14]. These images are 1.25 mm slice thick and captured by an individual inhale and exhale. The position of cancerous nodule is identified through the radiologists are also given in the dataset [15][16][17]. The information related to the dataset is offered in Table 1 and the sample images are demonstrated in Fig. 5. As seen in the table, it is noted that a total of 900 images were present where a set of 300 images falls under every level of 0, 1 and 2 respectively.

Table 1 Dataset Description

Description	Lung Database
Class count	3
Benign/Malignant/Normal	Label (0/1/2)
Benign image count	300
Malignant image count	300
Normal image count	300
Total image count	900

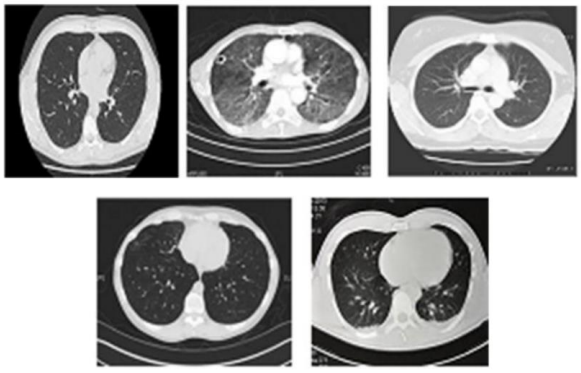

Fig. 5. Sample Database Images

A. Evaluation parameters

A set of measures used for the validation are sensitivity, specificity, accuracy, positive predictive value (PPV) and negative predictive value (NPV).

$$\text{Sensitivity} = \frac{TP}{TP + FN} \quad (8)$$

$$\text{Specificity} = \frac{TN}{TN + FP} \quad (9)$$

$$\text{Accuracy} = \frac{TP + TN}{TP + FP + FN + TN} \quad (10)$$

$$PPV = \frac{TP}{TP + FP} \quad (11)$$

$$NPV = \frac{TN}{TN + FN} \quad (12)$$

Where TP, TN, FP and FN indicates true positive, true negative, false positive and false negative correspondingly.

B. Results analysis

Fig. 6 shows the images produced by the pre-processing stage. Fig. 6b shows the image attained by the applied AHE model for enhancing the image contrast.

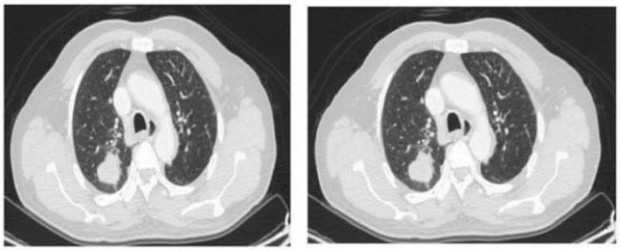

(a) (b)

Fig. 6 (a) Original Image (b) AHE image

Table 2 Visualization of Segmentation Results

Classes	Original Image	Segmented Image
Benign		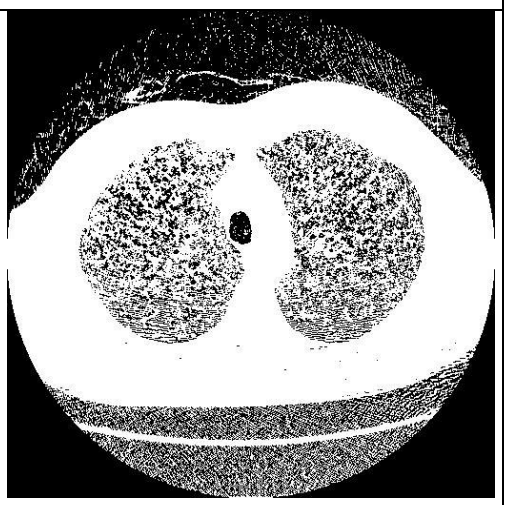
Malignant	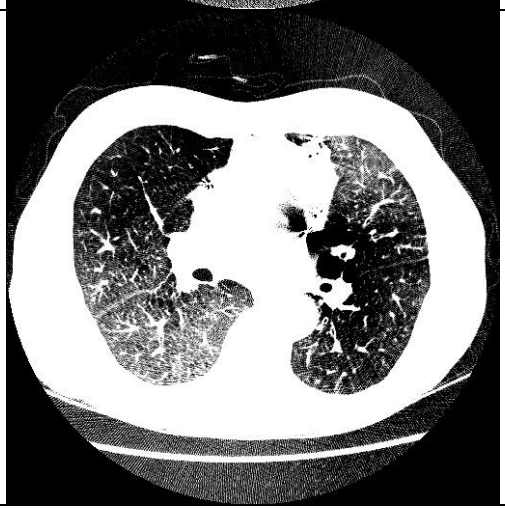	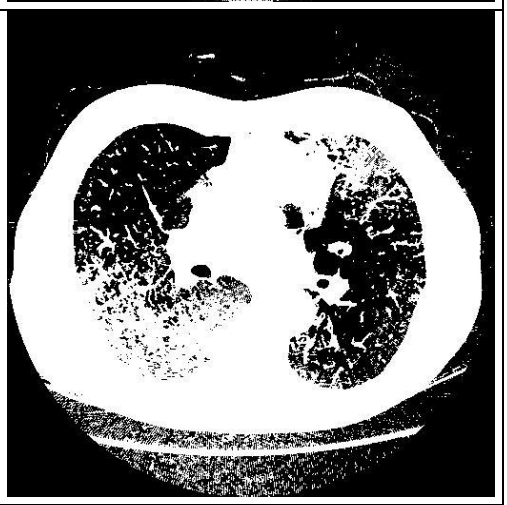

Normal	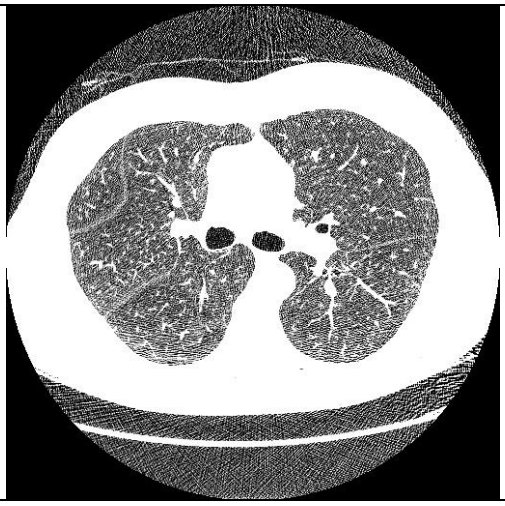	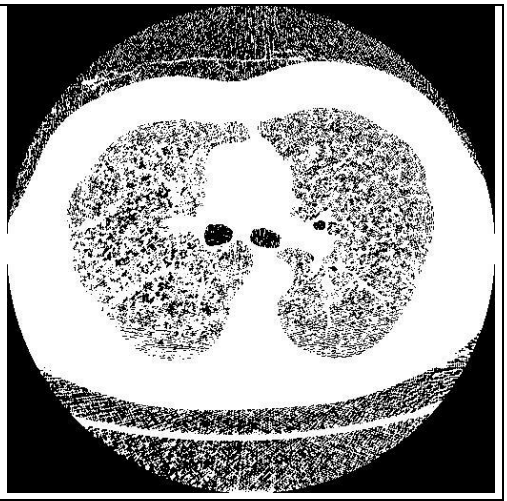

Table 3 provided the classification outcome by the LR model under different classes. The second row evidently denotes that the presented model precisely classifies the benign image as benign. Next, the third row obviously defines that the presented model accurately classifies the malignant image as malignant. The final row evidently denotes that the presented model precisely classifies the normal image as normal.

Table 3 Visualization of classifier results

Classes	Original Image	Classified Image
Benign	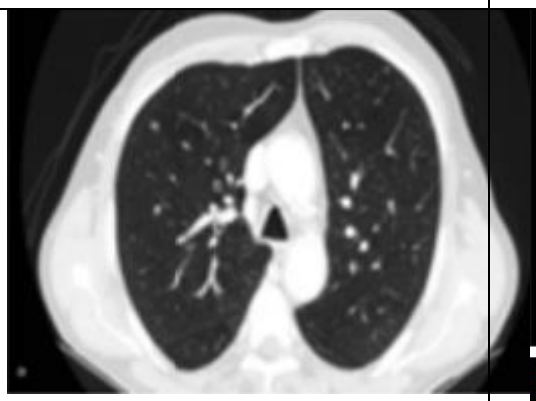	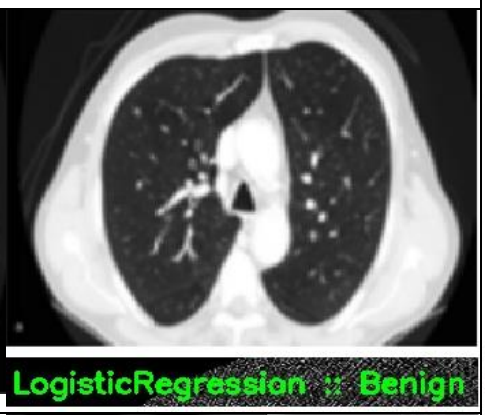
Malignant		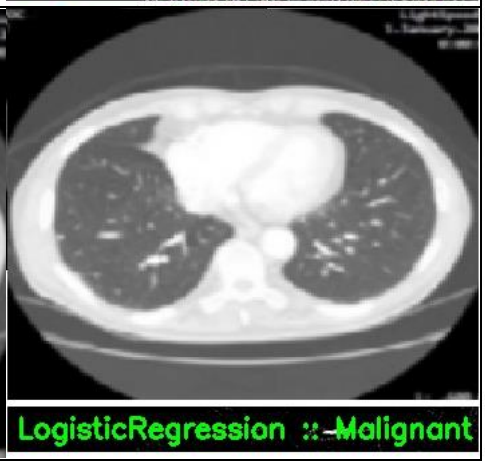

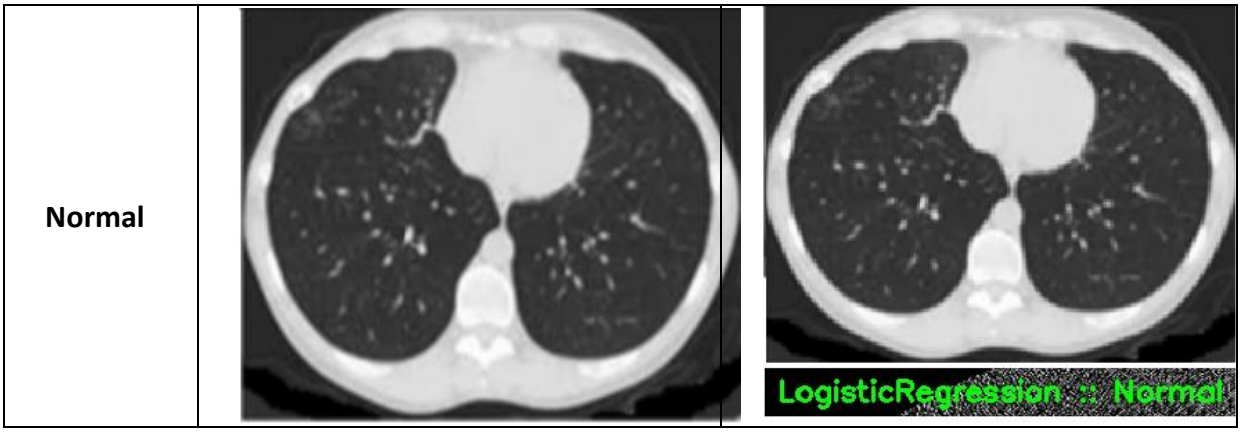

Fig. 7 offered the attained confusion matrix from classifier model. Among the total of 900 images, the presented model clearly classifies 295 images as benign, 294 images as malignant and 291 images as normal. The confusion matrix is derived in Table 4.

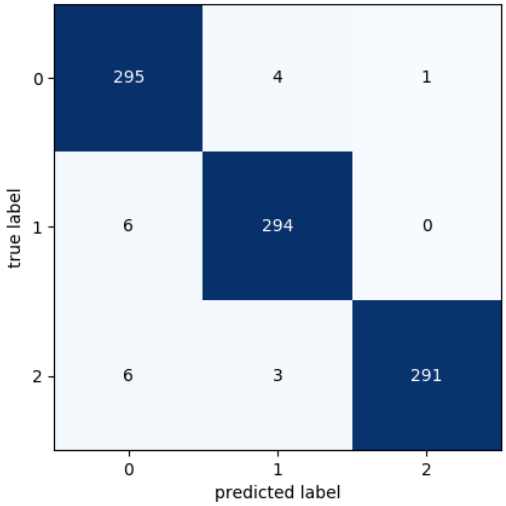

Fig. 7. Confusion matrix

Table 4 Derived Confusion Matrix

Input Label	Different Classes in Lung Cancer			Image count
	Benign	Malignant	Normal	
Benign	295	4	1	300
Malignant	6	294	0	300
Normal	6	3	291	300
Image count	307	301	292	900

To evaluate the effectiveness of the applied LR model, the generated 4×4 matrix undergo transformation to 2×2 matrix as given in Table 5.

Table 5 Manipulations from Confusion Matrix

Classes	Benign	Malignant	Normal
TP	295	294	291
TN	585	586	589
FP	12	7	1
FN	5	6	9

Table 6 and Fig. 8 display the results attained by the presented model interms of different measures. As shown, it is noted that the benign CT lung images are effectively classified with the sensitivity of 98.33, specificity of 97.99, accuracy of 98.10, PPV of 96.09 and NPV of 99.15. At the same time, it is observed that the malignant CT lung images are effectively classified with the sensitivity of 98, specificity of 98.82, accuracy of 98.54, PPV of 97.67 and NPV of 98.99. In the same way, the normal images are effectively classified with the sensitivity of 97, specificity of 99.89, accuracy of 98.88, PPV of 99.66 and NPV of 98.49. These values exhibited that the presented model shows effective classified under the normal CT lung images.

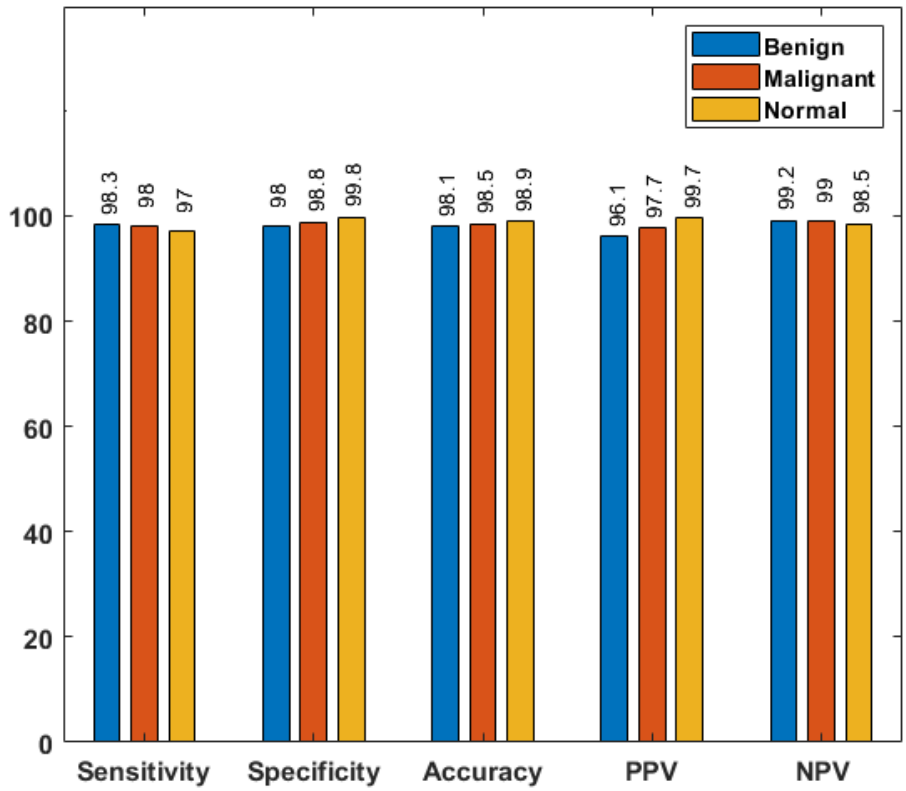

Fig. 8. Classifier results analysis under several measures

Table 6 Classifier results analysis under three classes

Classes	Sensitivity	Specificity	Accuracy	PPV	NPV
Benign	98.33	97.99	98.10	96.09	99.15
Malignant	98.00	98.82	98.54	97.67	98.99
Normal	97.00	99.83	98.88	99.66	98.49

Table 7 offered the comparative analysis of existing models with the presented one with respect to diverse measures. In addition, to clearly understand the betterment of the presented model, Figs. 9-11 visualize the comparative results of diverse models with respect to accuracy, sensitivity and specificity respectively.

Table 7 Comparative analysis of various methods in terms of Accuracy, Sensitivity and Specificity

Methods	Accuracy	Sensitivity	Specificity
Proposed	98.51	97.78	98.88
ODNN	94.56	96.20	94.20
MLP	82.00	77.00	72.00
RBF	84.00	86.00	54.00
Linear	77.00	89.00	36.00
ANN	86.00	87.00	79.00
KNN	91.00	90.00	83.00
DNN	87.65	82.43	89.67

Fig. 9 shows the accuracy analysis of diverse models on the classification of lung CT images. It can be seen that the linear regression model shows ineffective classification by attaining a minimum accuracy of 77. Likewise, the MLP classifier model attains moderate classification with the accuracy of 82. In the same way, the RBF model achieves slightly higher classification with accuracy of 84. Likewise, the ANN model obtains better classification accuracy of 86 over other models. In line with, the DNN model tried to manage well with the accuracy of 87.63. Next, the ODNN model exhibit competitive classification over the presented model by attaining the higher accuracy value of 94.56. However, maximum classification performance is attained by presented model with the accuracy of 98.51.

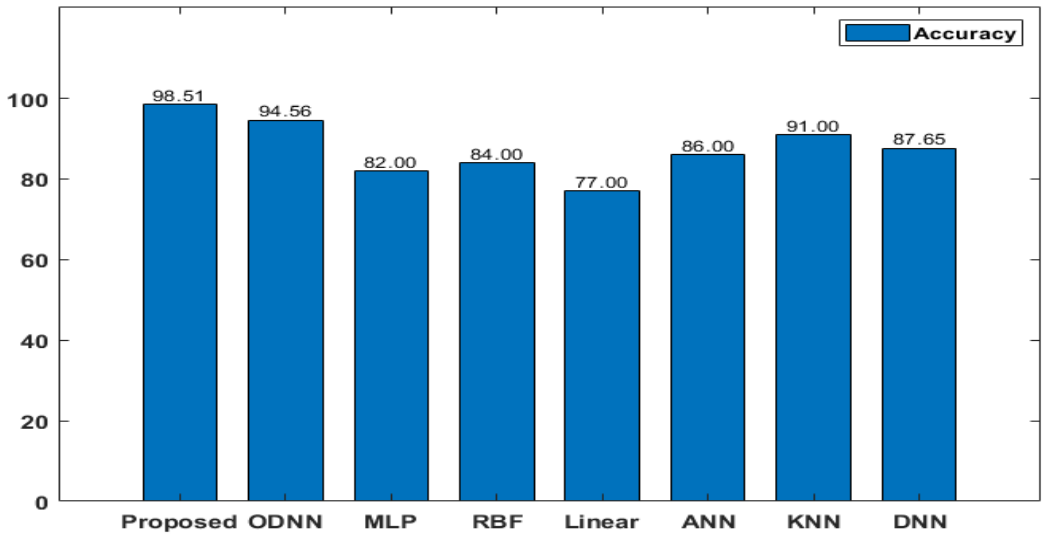

Fig. 9. Accuracy analysis of various models

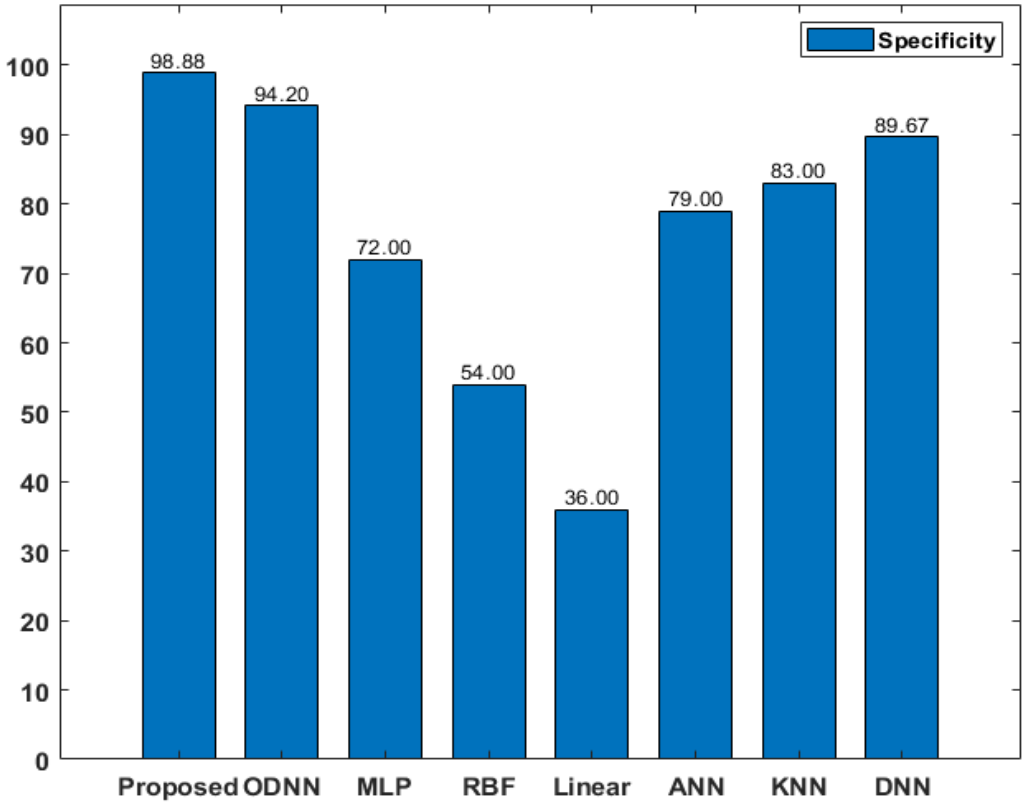

Fig. 10. Specificity analysis of various models

Fig. 10 shows the sensitivity analysis of diverse models on the classification of lung CT images. It can be seen that the MLP model shows ineffective classification by attaining a minimum sensitivity of 77. At the same time, the DNN classifier model attains moderate classification with the sensitivity of 82.43. In the same way, the RBF model achieves slightly higher classification with sensitivity of 86. Likewise, the ANN model obtains better classification sensitivity of 87 over other models. In line with, the linear regression model tried to manage well with the sensitivity of 89. Next, the ODNN model exhibit competitive classification over the presented model by attaining the higher sensitivity value of 96.30. However, maximum classification performance is attained by presented model with the sensitivity of 97.78.

Fig. 11 shows the specificity analysis of diverse models on the classification of lung CT images. It can be seen that the linear regression model shows ineffective classification by attaining a minimum specificity of 36. At the same time, the RBF classifier model attains moderate classification with the specificity of 54. In the same way, the MLP model achieves slightly higher classification with specificity of 72. Likewise, the ANN model obtains better classification specificity of 79 over other models. In line with, KNN model tried to manage well with the specificity of 83. Next, the ODNN model exhibit competitive classification over the presented model by attaining the higher specificity value of 94.20. However, maximum classification performance is attained by presented model with the specificity of 97.78.

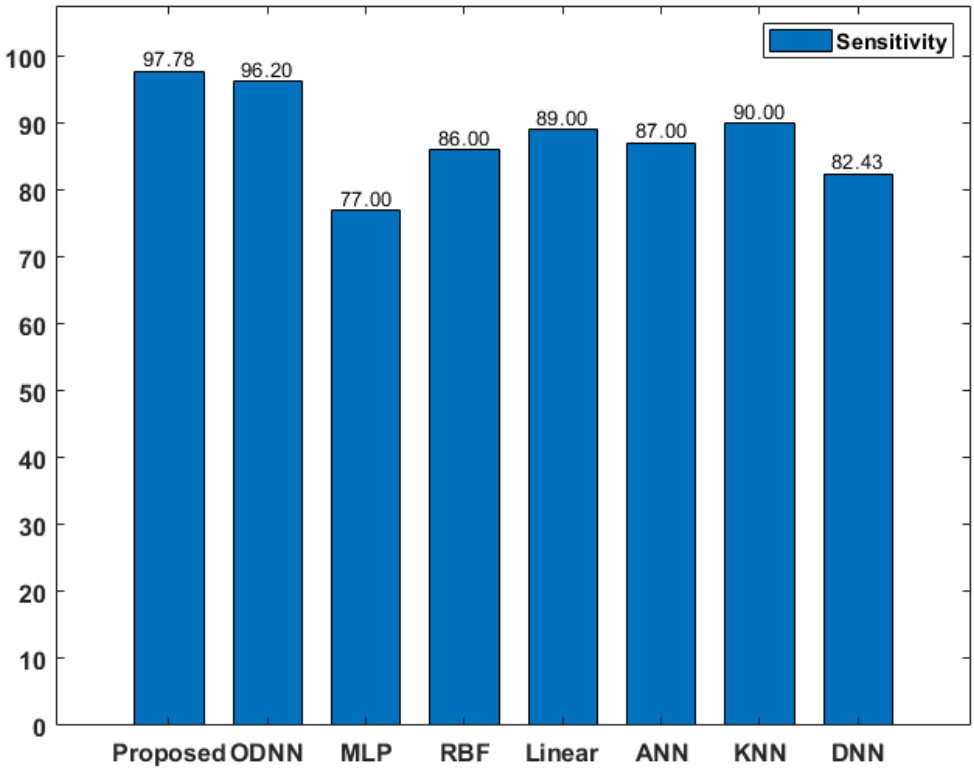

Fig. 11. Sensitivity analysis of various models

By looking into the above tables and figures, it is apparent that extraordinary classification of lung CT images is exhibited by the presented model by attaining the maximum sensitivity of 98.51, sensitivity of 97.88 and specificity of 98.88 respectively. These enhanced performances pointed out that it can be employed to test real time CT lung images.

III. CONCLUSION

Computer-aided diagnosis model finds useful for the professionally to detect and diagnose the abnormal images at the early stage and quickly. This paper has designed an effective diagnosis and classification model for CT lung images. The presented model involves different stages namely pre-processing, segmentation, feature extraction and classification. The pre-processing stage includes an AHE model for image enhancement and BF model for noise removal. The pre-processed images are fed into the second stage of watershed segmentation model for effectively segment the images. Then, a deep learning based Xception model is applied for prominent feature extraction and the classification takes place by the use of LR classifier. In this study, a benchmark lung cancer CT image dataset is utilized which comprises a set of fifty 50 low-dosage images. The presented model attains a maximum sensitivity of 98.51, sensitivity of 97.88 and specificity of 98.88 respectively. These enhanced performances pointed out that it can be employed to test real time CT lung images.

REFERENCES

1. S. Rattan, S. Kaur, N. Kansal, J. Kaur, An optimized lung cancer classification system for computed tomography images, in: Image Information Processing (ICIIP), 2017 Fourth International Conference on, IEEE, 2017, pp. 1–6.
2. P. Naresh, R. Shettar, Image processing and classification techniques for early detection of lung cancer for preventive health care: a survey, Int. J. Recent Trends Eng. Tech. 11 (1) (2014) 595.
3. F.C. Detterbeck, Lung Cancer Stage Classification: What Does It Mean on Main Street, eighth ed., 2017, pp. 1–26.
4. Y. Xie, J. Zhang, Y. Xia, M. Fulham, Y. Zhang, Fusing texture, shape and deep model-learned information at decision level for automated classification of lung nodules on chest ct, Information Fusion 42 (2018) 102–110.
5. H. Chougrad, H. Zouaki, O. Alheyane, Deep convolutional neural networks for breast cancer screening, Comput. Methods Programs Biomed. 157 (2018) 19– 30.
6. H. Mohsen, E.S.A. El-Dahshan, E.S.M. El-Horbaty, A.B.M. Salem, Classification using deep learning neural networks for brain tumors, Future Comput. Inf. J. (2017)
7. A. Sharma, K.K. Paliwal, A deterministic approach to regularized linear discriminant analysis, Neurocomputing 151 (2015) 207–214.
8. S. Nagpal, S. Arora, S. Dey, Feature selection using gravitational search algorithm for biomedical data, Proc. Comput. Sci. 115 (2017) 258–265.
9. S.K. Lakshmanaprabu, K. Shankar, A. Khanna, D. Gupta, J.J. Rodrigues, P.R. Pinheiro, V.H.C. De Albuquerque, Effective features to classify big data using social internet of things, IEEE Access 6 (2018) 24196–24204.
10. J. Kuruvilla, K. Gunavathi, Lung cancer classification using neural networks for CT images, Comput. Methods Programs Biomed. 113 (1) (2014) 202–209
11. Z. Wang, J. Tao, A fast implementation of adaptive histogram equalization, in: Signal Processing, 2006 8th International Conference on, vol. 2, IEEE, 2006, pp. 1–4.
12. C. Ahlstrom, P. Hult, P. Rask, J.E. Karlsson, E. Nylander, U. Dahlstrom, P. Ask, Feature extraction for systolic heart murmur classification, Annals of Biomedical Engineering 34 (November (11)) (2006) 1666–1677.
13. Chollet, F., 2017. Xception: Deep learning with depthwise separable convolutions. In *Proceedings of the IEEE conference on computer vision and pattern recognition* (pp. 1251-1258).
14. http://www.via.cornell.edu/lungdb.html
15. K.Seetharaman, S.Sathiamoorthy, Mar 2014, "Color image retrieval using statistical model and radial basis function neural network.", Egyptian Informatics Journal, Vol. 15, No. 1, pp. 59-68.
16. K.Seetharaman, S.Sathiamoorthy, A Unified Learning Framework for Content Based Medical Image Retrieval Using a Statistical Model. Journal of King Saud University - Computer and Information Sciences, Vol. 28 (2016), No. 1, Dec 2015, pp. 110-124.
17. M. Kamarasan, S.Sathiamoorthy, 2014, Content based Intelligent Image Retrieval Based on Super Pixel with Wavelet Transform, International Journal of Innovative Research in Science, Engineering and Technology, 3(5):13068-13075.